Egypt. J. Chem. **Vol. 67**, No. 2 pp. 199 - 204 (2024)

Egyptian Journal of Chemistry

http://ejchem.journals.ekb.eg/

Role of Silver Nanoparticles on the Structure and Optical Properties of CS/PVP/AMOX Nanocomposites

S. Ebrahim[a]*, A.M. Abdelghany[b], D.M. Ayad[a], M.Y. Abdelaal[a]

[a]Chemistry Department, Faculty of Science, Mansoura University, Mansoura, 35516, Egypt
[b]Spectroscopy Department, Physics Research Institute, National Research Center, 33 Elbehouth St., 12311, Dokki, Giza, Egypt

Abstract

Silver nanoparticles (AgNPs) were successfully synthesized via laser ablation technique in aqueous media. Polymer blends of Chitosan (CS), polyvinylpyrrolidone (PVP), and Amoxicillin (AMOX) were synthesized using a casting technique from a common solvent. Ag NPs were incorporated into CS/PVP/AMOX blend matrix to outline the role played by AgNPs on the blend's main characteristics. Synthesized nanoparticles show a surface plasmon resonance peak at about 430 nm. XRD pattern of the synthesized silver reveals the formation of homogenous multi-dispersed nanoparticles with an average size of 14 nm calculated using the Scherrer equation and with an agreement with that obtained from transmission electron microscopic (TEM) image. The optical energy gap is calculated from the electronic UV/Vis. transitions in combination with the measured electrical conductivity of the studied samples imply a composition dependence on the obtained values. The antibacterial effect of the samples was measured, which shows a correlation with the added amount of the dopant materials.

Keywords: Chitosan (CS); PVP; Silver nanoparticles (AgNPs); Optical parameters; Laser ablation.

1. Introduction

Polymer blending attracts the curiosity of several scientists within the last decades because of their superior characteristics among their separate polymer networks and wide applications [1-3]. In addition, doping polymeric matrices with inorganic materials [4] or nanomaterials [5] may result in new applications. The development of biomaterials and drug delivery systems has sparked a lot of attention as the demand for millennium goals results from low cost and ease of production [6, 7]. The biocidal action of silver nanoparticles takes place by the slow liberation of Ag^+ and by several mechanisms like reaction with thiols groups in enzymes and proteins, inducement of oxidative agents, and inhibition of DNA, leading to the difficulty of the production of resistant strains by bacteria. In addition to that, the large surface area of silver nanoparticles enhances the reactivity and sorption with pathogens [8].

Because of its high environmental stability, simple processability, reasonable electrical conductivity, and diverse physics in charge transport mechanism, PVP remains crucial among the conjugated polymers. Because of the existence of the stiff pyrrolidone group, it is an amorphous polymer with high glass transition temperatures (Tg) up to 170 °C. It has great wetting capabilities in solution and rapidly forms films. This makes it suitable for use as a coating or as a coating additive [9, 10].

Chitosan is a positively charged natural polysaccharide, which is composed of β-(1→4)-linked N-acetyl-D-glucosamine (GlcNAc) and D-glucosamine (GlcN) [11]. Chitosan is derived from the deacetylation of chitin polymer, and it is soluble

*Corresponding author e-mail: samarebrahim@mans.edu.eg.; (Samar Ebrahim)
Received date 01 June 2023; revised date 05 July 2023; accepted date 31 July 2023
DOI: 10.21608/EJCHEM.2023.214816.8067

in acidic aqueous media because of the existence of amino groups Chitosan has a high ability to form films, but biopolymers are more expensive than synthetic polymers. So, to overcome that, blending between natural and synthetic polymers introduces new substances with improved characteristics with reduced costs [12]

Amoxicillin drug is one of the most common antibiotics which are used to treat the eradication caused by Helicobacter pylori (H. pylori) which is a Gram-negative bacterium. Nanoencapsulation of drugs is a novel therapeutic technique to retard infections caused by bacteria. As a result of that, amoxicillin has been encapsulated in several forms in drug delivery systems like gastro-retentive tablets, polymeric, and lipid nanoparticles [13,14].

The present study is aiming to correlate the role of AgNPs embedded within blends of CS/PVP/AMOX thin films on their conductivity.

2. Experimental

2.1.Sample preparation

Parent undoped thin films of Chitosan/ Polyvinylpyrrolidone (CS/PVP) (75/25wt%) in addition to another sample that doped with minor concentrations of variable mass fractions of AMOX and AgNPs were successfully synthesized via traditional solution casting route. Silver nanoparticles (AgNPs) were successfully synthesized *via* the laser ablation route in aqueous media. Clean Silver target immersed in distilled water subjected for Nd:YAG nanosecond pulsed laser adopting 1064 nm beam of width 6 nm and power 4 Watt with pulse frequency 10Hz [15].

2.2. Preparation of CS/PVP (S0)

A blend of CS/PVP was prepared by dissolving about 0.75 g of CS in 125 ml of 2% aqueous acetic acid and 0.25 g of PVP in 25 ml of distilled water. The two polymeric solutions were mixed by continuous stirring till the solution became homogeneous. After that, 25 ml of the blend solution which contain about 0.167 g of CS and PVP was cast on a plastic Petri dish and dried in an oven regulated at 50°C for 24h.

2.3. Preparation of CS/PVP/AMOX/AgNPs samples (S2 and S4)

Samples were synthesized by adding different mass fractions of AMOX and AgNPs to 25 ml of the blend solution containing about 0.167 g of CS/PVP blend as shown in Table 1, casting on clean plastic Petri dishes and drying in an oven at 50 °C for 24h.

Table 1: Amount of AMOX and AgNPs in S0, S1, and S2 composites

Samples* CS/PVP	Amount (mg)	
	AMOX	AgNPs
S0	0	0
S2	133	0.16
S4	266	0.32

*****All samples contain about 0.167 g of CS:PVP blend

2.4. Synthesis of silver nanoparticles

The experimental configuration used to create Ag colloids using laser ablation. The silver plate was set on the bottom of a glass jar that was filled with deionized and redistilled ultrapure water (>99.9% purity). A two-millimeter-thick coating of water was spread thinly across the silver foil. An ultrasonic bath was utilized to clean a silver plate and an ablation cell before laser ablation. During the ablation and fragmentation processes, the solution was gradually swirled.

An outdoor (aerobic) environment was used for the preparation. Silver colloid was created using an active Q-Switched Nd:YAG laser system with a pulse width of 20 ns and a repetition rate of 5 Hz. An optical power detector was used to measure optical power, and a control voltage was set for the laser lamp discharge. With an aperture to control the size of the unfocused laser light's spot, the laser beam's core section was selected. The Nd:YAG laser's fundamental (1064 nm) and second harmonic (532 nm) outputs were utilized as an irradiation source.

3. Characterization of prepared compounds

X-ray diffraction scans (XRD) recorded with a (PAN analytical X' Pert PRO XRD system) occupied with Cu K radiation (λ= 1.540) with a tube operating voltage of approximately 30 kV, Bragg's angle (2θ) extended from (5 to 80 °C) at STP, and the diameter of the incident beam can reach 100m were used to identify the crystalline/amorphous forms of the samples. Jasco 750 UV/Vis double beam spectrophotometer was used to record the spectral data within the range 200-1100nm. The size of the synthesized nanoparticles was examined using transmission electron microscopy (TEM) Model TEM-2100 JEOL, Japan. The DC electrical conductivity was recorded using two probe

arrangements adopting the KETHLEY 6517B electrometer, USA with an accuracy of ±0.5%. The antibacterial activity of the synthesized samples and AMOX was tested against gram-positive bacteria (Staphylococcus aureus), and Gram-negative bacteria (Escherichia coli). The % activity index for the complex was calculated by the formula:

$$\%\ Activity\ Index = \frac{Zone\ of\ inhibition\ by\ test\ compound\ (diametre)}{Zone\ of\ inhibition\ by\ standard\ (diametre)} \times 100$$

4. Results and Discussion

4.1. Characterization of synthesized silver nanoparticles

Figure (1) reveals the UV/Vis. Optical absorption spectral data of the synthesized silver nanoparticles. Obtained data shows the presence of a broad less intense peak centered at about 420 nm usually assigned to the characteristic surface plasmon resonance (SPR) of silver nanoparticles (AgNPs) previously reported by several authors [16]. In addition, the obtained transmission electron microscope image shows the presence of AgNPs with an average size ranging between 70-80 nm.

Figure (2) displays the X-ray diffraction pattern (XRD) of the studied silver nanoparticles. Several sharp peaks at Bragg angles 38, 44.5, 65.5, and 78° correspond to (111), (200), (220), and (311) in agreement with that reported for the face-cantered cubic (fcc) structure of silver (JCPDS file No. 04-0783) [17].

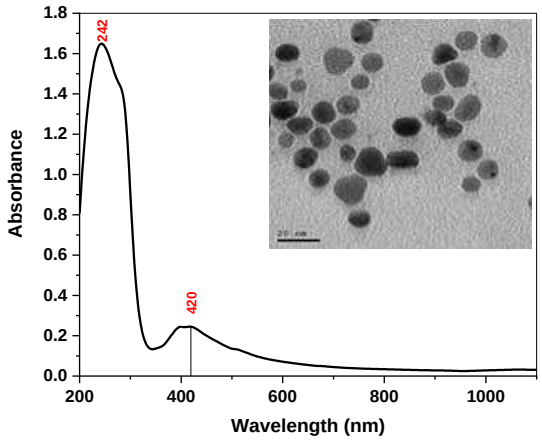

Figure (1): UV/Vis. optical absorption spectrum of the synthesized AgNPs combined with TEM microscopic image

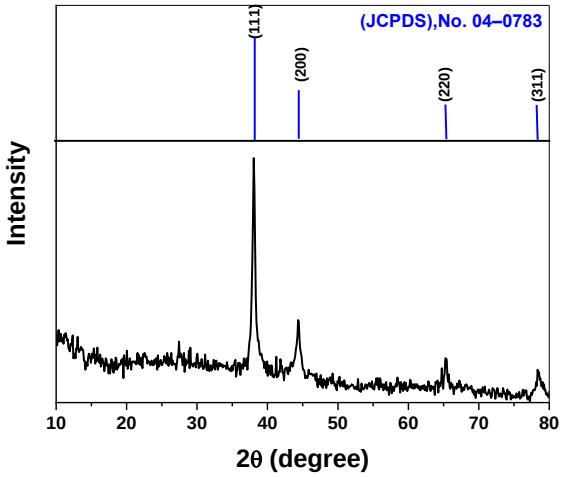

Figure (2): X-ray diffraction pattern (XRD) of the green synthesized silver nanoparticles.

4.2. UV/Vis of the synthesized samples

Figure (3a-c) shows the UV/Vis. electronic transition of the studied samples along with the direct and indirect transitions. Obtained spectra show a strong charge transfer band located at 230, 233, and 234 nm for S0, S2, and S4 respectively attributed to n→π* transition. In addition, the optical energy gap can be calculated using the wavelength λ_{edge} in the intersection of the fundamental absorption edge with the x-axis using the formula; $E_g = h\ c/\lambda_{edge}$ and by using Tauc's plot to represent the relation between $[(\alpha h\nu)^{\frac{1}{2}}$ and $(\alpha h\nu)^2]$ versus photon energy hν. In both direct and indirect transitions, the energy gap Eg at the X-axis intercept may be determined [18-20].

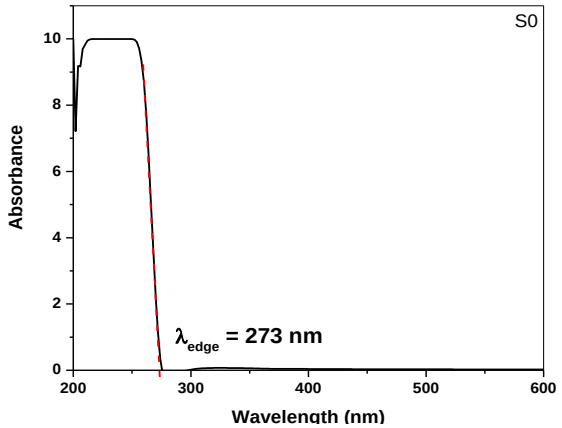

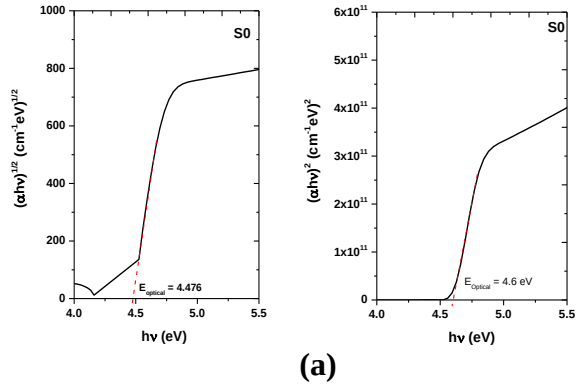

(a)

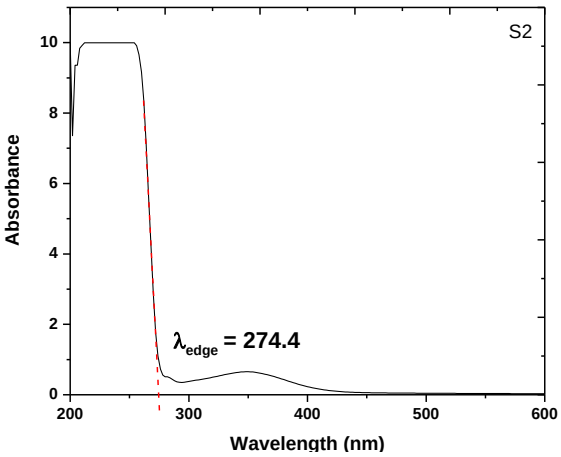

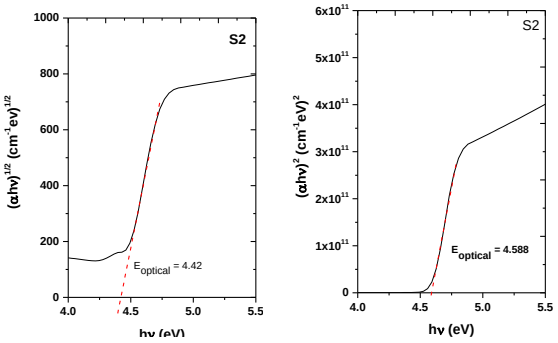

(b)

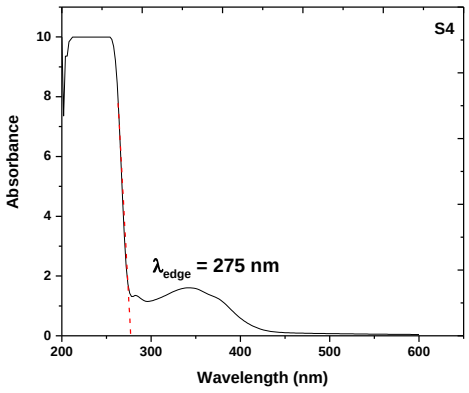

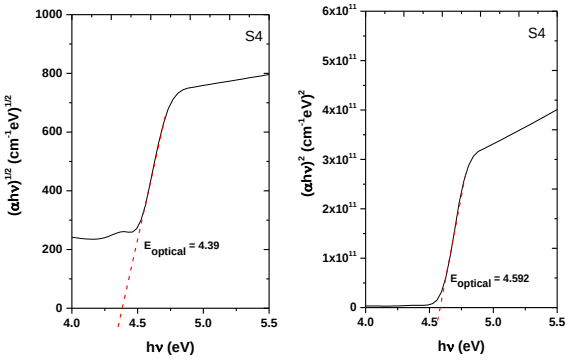

(c)

Figure (3): UV/Vis. electronic transition of S0-S4 samples along with the direct and indirect transitions.

4.3. Electrical conductivity

The electrical conductivity was calculated for samples of nearly the same thickness (0.2 mm) coated with the silver electrode of 1 cm^2 area. Direct current conductivity (DC) is calculated using the formula (σ = d/RA), where A is the electrode area and d is the sample thickness. Calculated data were tabulated in Table 2. It was recognized that electrical conductivity increased with the addition of both AMOX and AgNPs due to the conducting nature of both dopant materials.

Table 2: electrical conductivity results of S0, S2, and S4

Samples	Electrical conductivity (σS/cm)
S0	1.92×10^{-10}
S2	1.11×10^{-6}
S4	9.67×10^{-6}

4.4. Antibacterial study

Table 3 shows the antibacterial activity of the synthesized samples against gram-positive bacteria (*Staphylococcus aureus*), and Gram-negative bacteria (*Escherichia coli*). Sample S0, which is free from drugs and AgNPs, shows no activity against the two types of bacteria. The antibacterial effect appears in samples S2 and S4, due to the release of AMOX and AgNPs from the polymeric matrices and effectively inhibited the target bacteria. The antibacterial effect of AMOX takes place by inhibiting the formation of the cell wall of bacteria, which this cell wall protects the bacteria from their outside environment [21]. The antibacterial effect of AgNPs was explained by the interaction of the silver (Ag^+) ions with the thiol (-

SH) group of amino acids like cysteine that exist in the proteins which belong to the respiratory enzyme class and this causes the destruction of the respiratory system of the bacterial cells and finally leads to the death of the bacterial cell [22].

Table 3: The antibacterial activity of S0-S4 samples against two types of bacteria (*E. coli* and *S. aureus*)

samples	*E. coli* (mg/ml)		*S. aureus* (mg/ml)	
	D (mm)	**Act. index %**	**D (mm)**	**Act. index %**
S0	NA	----	NA	----
S2	3	11.5	9	37.5
S4	13	50	13	54.2
AgNPs	9	34.6	16	66.7
AMOX	26	100	24	100

Where D is the diameter of the inhibition zone

5. Conclusions

Flexible thin films of 75 wt% chitosan (CS) and 25wt% Polyvinylpyrrolidone (PVP) with silver nanoparticles (AgNPs) and amoxicillin drug (AMOX) with variable mass fraction were successfully synthesized. Effect of dopant (AgNPs) concentration on the electrical conductivity of the samples was studied. It increases by increasing the AgNPs concentration, due to the decrease in the distance between AgNPs in the polymeric matrices. Although the antibacterial activity of CS/PVP thin film was enhanced by the addition of AMOX and AgNPs, due to their effective antibacterial activity. Therefore, studied samples can be utilized in versatile medical and electrochemical applications.

6. Conflicts of interest

The authors declared that there is no conflict of interest.

7. Formatting of funding sources

Authors receive no funding.

8. References

[1] Ahmed, H. T. & Abdullah, O. G. (2019). Preparation and composition optimization of PEO: MC polymer blend films to enhance electrical conductivity. Polymers, 11(5), 853.

[2] Kawaguchi, M. (2017). Interfacial characteristics of binary polymer blend films spread at the air-water interface. Advances in colloid and interface science, 247, 163-171.

[3] Al-Shamari, A. A., Abdelghany, A. M., Alnattar, H., & Oraby, A. H. (2021). Structural and optical properties of PEO/CMC polymer blend modified with gold nanoparticles synthesized by laser ablation in water. Journal of Materials Research and Technology, 12, 1597-1605.

[4] Spirescu, V. A., Chircov, C., Grumezescu, A. M., Vasile, B. Ș., & Andronescu, E. (2021). Inorganic Nanoparticles and Composite Films for Antimicrobial Therapies. International Journal of Molecular Sciences, 22(9), 4595.

[5] Alonso, Y. N., Grafia, A. L., Castillo, L. A., & Barbosa, S. E. (2021). Active packaging films based on polyolefins modified by organic and inorganic nanoparticles. In Reactive and Functional Polymers Volume Three (pp. 5-28). Springer, Cham.

[6] Hashim, A., & Habeeb, M. A. (2019). Synthesis and characterization of polymer blend-$CoFe_2O_4$ nanoparticles as a humidity sensors for different temperatures. Transactions on Electrical and Electronic Materials, 20(2), 107-112.

[7] Lo, L. W., Zhao, J., Wan, H., Wang, Y., Chakrabartty, S., & Wang, C. (2021). An Inkjet-Printed PEDOT: PSS-Based Stretchable Conductor for Wearable Health Monitoring Device Applications. ACS Applied Materials & Interfaces, 13(18), 21693-21702.

[8] Yu, S. J., Yin, Y. G., & Liu, J. F. (2013). Silver nanoparticles in the environment. Environmental Science: Processes& Impacts,15(1), 78-92.

[9] Sazali, N., Salleh, W. N. W., Ismail, A. F., & Iwamoto, Y. (2021). Incorporation of thermally labile additives in polyimide carbon membrane for hydrogen separation. International Journal of Hydrogen Energy, 46(48), 24855-24863.

[10] Jothi, M. A., Vanitha, D., Bahadur, S. A., & Nallamuthu, N. (2021). Promising biodegradable polymer blend electrolytes based on cornstarch: PVP for electrochemical cell applications. Bulletin of Materials Science, 44(1), 1-12.

[11] Li, J., Cai, C., Li, J., Li, J., Li, J., Sun, T., & Yu, G. (2018). Chitosan-based nanomaterials for drug delivery.*Molecules*,*23*(10), 2661.

[12] Pavaloiu, R. D., Stoica-Guzun, A., Stroescu, M., Jinga, S. I., & Dobre, T. (2014). Composite films of poly(vinyl alcohol)–chitosan–bacterial cellulose for drug controlled release. International Journal of Biological Macromolecules, 68, 117-124.

[13] Abdelghany, A., El-Desouky, M. A., & Shemis,

M. (2021). Synthesis and characterization of amoxicillin-loaded polymeric nanocapsules as a drug delivery system targeting Helicobacter pylori.*Arab Journal of Gastroenterology*,*22*(4), 278-284.

[14] Paloma, M., Enobakhare, Y., Torrado, G., & Torrado, S. (2003). Release of amoxicillin from polyionic complexes of chitosan and poly (acrylic acid). Study of polymer/polymer and polymer/drug interactions within the network structure.*Biomaterials*,*24*(8), 1499-1506.

[15] Menazea, A. A., & Awwad, N. S. (2020). Pulsed Nd: YAG laser deposition-assisted synthesis of silver/copper oxide nanocomposite thin film for 4-nitrophenol reduction. Radiation Physics and Chemistry, 177, 109112.

[16] Ahmadpourian, A. et al. (2016). The effects of deposition time on surface morphology, structural, electrical and optical properties of sputtered Ag-Cu thin films. Eur Phys J Plus,131(10), 1-7.

[17] Agasti, N. & Kaushik, N.K. (2014). One-pot synthesis of crystalline silver nanoparticles. Amer J Nanomater,2(1), 4-7.

[18] Mott, N. F., & Davis, E. A. (2012). Electronic processes in non-crystalline materials. Oxford University Press.

[19] Coulter, J. B. & Birnie III, D. P. (2018). Assessing Tauc plot slope quantification: ZnO thin films as a model system. Physica Status Solidi (B), 255, 1700393.

[20] Hammad, A. H. & Abdelghany, A. M. (2016). Optical and structural investigations of zinc phosphate glasses containing vanadium ions. J Non-Cryst Solids, 433, 14-19.

[21] Bebu, A., Szabó, L., Leopold, N., Berindean, C., & David, L. (2011). IR, Raman, SERS and DFT study of amoxicillin. Journal of Molecular Structure 993, 52-56.

[22] Dara, P. K., Mahadevan, R., Digita, P. A., Visnuvinayagam, S. L., Kumar, R. G., Mathew, S., Ravishankar, C. N., & Anandan, R. (2020). Synthesis and biochemical characterization of silver nanoparticles grafted chitosan (Chi-Ag-NPs): in vitro studies on antioxidant and antibacterial applications. SN Applied Sciences, 2, 665.